

Control of Complex Maneuvers for a Quadrotor UAV using Geometric Methods on $SE(3)$

Taeyoung Lee*, Melvin Leok[†], and N. Harris McClamroch

Abstract—This paper provides new results for control of complex flight maneuvers for a quadrotor unmanned aerial vehicle (UAV). The flight maneuvers are defined by a concatenation of flight modes or primitives, each of which is achieved by a nonlinear controller that solves an output tracking problem. A mathematical model of the quadrotor UAV rigid body dynamics, defined on the configuration space $SE(3)$, is introduced as a basis for the analysis. The quadrotor UAV has four input degrees of freedom, namely the magnitudes of the four rotor thrusts; each flight mode is defined by solving an asymptotic optimal tracking problem. Although many flight modes can be studied, we focus on three output tracking problems, namely (1) outputs given by the vehicle attitude, (2) outputs given by the three position variables for the vehicle center of mass, and (3) output given by the three velocity variables for the vehicle center of mass. A nonlinear tracking controller is developed on the special Euclidean group $SE(3)$ for each flight mode, and the closed loop is shown to have desirable properties that are almost global in each case. Several numerical examples, including one example in which the quadrotor recovers from being initially upside down and another example that includes switching and transitions between different flight modes, illustrate the versatility and generality of the proposed approach.

I. INTRODUCTION

A quadrotor unmanned aerial vehicle (UAV) consists of two pairs of counter-rotating rotors and propellers, located at the vertices of a square frame. It is capable of vertical take-off and landing (VTOL), but it does not require complex mechanical linkages, such as swash plates or teeter hinges, that commonly appear in typical helicopters. Due to its simple mechanical structure, it has been envisaged for various applications such as surveillance or mobile sensor networks as well as for educational purposes. There are several university-level projects [1], [2], [3], [4], and commercial products [5], [6], [7] related to the development and application of quadrotor UAVs.

Despite the substantial interest in quadrotor UAVs, little attention has been paid to constructing nonlinear control systems that can achieve complex aerobatic maneuvers. Linear control systems such as proportional-derivative controllers or linear quadratic regulators are widely used to enhance the stability properties of an equilibrium [1], [3], [4], [8], [9]. A nonlinear controller is developed for the linearized dynamics of a quadrotor UAV in [10]. Backstepping and sliding mode

techniques are applied in [11]. Since all of these controllers are based on Euler angles, they exhibit singularities when representing complex rotational maneuvers of a quadrotor UAV, thereby significantly restricting their ability to achieve complex flight maneuvers.

Geometric control, as utilized in this paper, is concerned with the development of control systems for dynamic systems evolving on nonlinear manifolds that cannot be globally identified with Euclidean spaces [12], [13], [14]. By characterizing geometric properties of nonlinear manifolds intrinsically, geometric control techniques provide unique insights into control theory that cannot be obtained from dynamic models represented using local coordinates [15]. This approach has been applied to fully actuated rigid body dynamics on Lie groups to achieve almost global asymptotic stability [14], [16], [17], [18].

In this paper, we make use of geometric methods to define and analyze controllers that can achieve complex aerobatic maneuvers for a quadrotor UAV. The dynamics of the quadrotor UAV are expressed globally on the configuration manifold, which is the special Euclidean group $SE(3)$. Based on a hybrid control architecture, we construct controllers that can achieve output tracking for outputs that correspond to each of several flight modes. In particular, we introduce three flight modes, each defined by a nonlinear controller that achieves: (1) almost global asymptotic tracking of the attitude of the quadrotor UAV, (2) almost global asymptotic tracking of the position of the center of mass of the quadrotor UAV, and (3) almost global asymptotic tracking of the velocity of the center of mass of the quadrotor UAV. Since the control approach is coordinate-free, it completely avoids singularities and complexities that arise when using local coordinates.

The paper is organized as follows. We develop a globally defined model for the translational and rotational dynamics of a quadrotor UAV in Section II. The hybrid control architecture and three flight modes are introduced in Section III. Section IV presents results for the attitude controlled flight mode; Sections V and VI present results for the position controlled flight mode, and the velocity controlled flight mode, respectively. Several numerical results that demonstrate complex aerobatic maneuvers for a typical quadrotor UAV are presented in Section VII.

II. QUADROTOR DYNAMICS MODEL

Consider a quadrotor UAV model illustrated in Figure 1. This is a system of four identical rotors and propellers located at the vertices of a square, which generate a thrust and torque normal to the plane of this square. We choose an inertial reference frame $\{\vec{e}_1, \vec{e}_2, \vec{e}_3\}$ and a body-fixed frame

Taeyoung Lee, Mechanical and Aerospace Engineering, Florida Institute of Technology, Melbourne, FL 32901 taeyoung@fit.edu

Melvin Leok, Mathematics, University of California at San Diego, La Jolla, CA 92093 mleok@math.ucsd.edu

N. Harris McClamroch, Aerospace Engineering, University of Michigan, Ann Arbor, MI 48109 nhm@umich.edu

*This research has been supported in part by NSF under grants CMMI-1029551.

[†]This research has been supported in part by NSF under grants DMS-0726263, DMS-100152 and DMS-1010687.

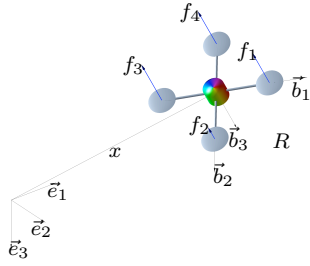


Fig. 1. Quadrotor model

$\{\vec{b}_1, \vec{b}_2, \vec{b}_3\}$. The origin of the body-fixed frame is located at the center of mass of this vehicle. The first and the second axes of the body-fixed frame, \vec{b}_1, \vec{b}_2 , lie in the plane defined by the centers of the four rotors, as illustrated in Figure 1. The third body-fixed axis \vec{b}_3 is normal to this plane. Each of the inertial reference frame and the body-fixed reference frame consist of a triad of orthogonal vectors defined according to the right hand rule. In the subsequent development, these references frames are taken as basis sets and we use vectors in \mathbb{R}^3 to represent physical vectors and we use 3×3 real matrices to represent linear transformations between the vector spaces defined by these two frames. Define

$m \in \mathbb{R}$	the total mass
$J \in \mathbb{R}^{3 \times 3}$	the inertia matrix with respect to the body-fixed frame
$R \in \text{SO}(3)$	the rotation matrix from the body-fixed frame to the inertial frame
$\Omega \in \mathbb{R}^3$	the angular velocity in the body-fixed frame
$x \in \mathbb{R}^3$	the position vector of the center of mass in the inertial frame
$v \in \mathbb{R}^3$	the velocity vector of the center of mass in the inertial frame
$d \in \mathbb{R}$	the distance from the center of mass to the center of each rotor in the \vec{b}_1, \vec{b}_2 plane
$f_i \in \mathbb{R}$	the thrust generated by the i -th propeller along the $-\vec{b}_3$ axis
$\tau_i \in \mathbb{R}$	the torque generated by the i -th propeller about the \vec{b}_3 axis
$f \in \mathbb{R}$	the total thrust magnitude, i.e., $f = \sum_{i=1}^4 f_i$
$M \in \mathbb{R}^3$	the total moment vector in the body-fixed frame

The configuration of this quadrotor UAV is defined by the location of the center of mass and the attitude with respect to the inertial frame. Therefore, the configuration manifold is the special Euclidean group $\text{SE}(3)$, which is the semidirect product of \mathbb{R}^3 and the special orthogonal group $\text{SO}(3) = \{R \in \mathbb{R}^{3 \times 3} \mid R^T R = I, \det R = 1\}$.

The following conventions are assumed for the rotors and propellers, and the thrust and moment that they exert on the quadrotor UAV. We assume that the thrust of each propeller is directly controlled, i.e., we do not consider the dynamics of rotors and propellers, and the direction of the thrust of each propeller is normal to the quadrotor plane. The first and third propellers are assumed to generate a thrust along the direction of $-\vec{b}_3$ when rotating clockwise; the second and fourth propellers are assumed to generate a thrust along the

same direction of $-\vec{b}_3$ when rotating counterclockwise. Thus, the thrust magnitude is $f = \sum_{i=1}^4 f_i$, and it is positive when the total thrust vector acts along $-\vec{b}_3$, and it is negative when the total thrust vector acts along \vec{b}_3 . By the definition of the rotation matrix $R \in \text{SO}(3)$, the total thrust vector is given by $-fRe_3 \in \mathbb{R}^3$ in the inertial frame. We also assume that the torque generated by each propeller is directly proportional to its thrust. Since it is assumed that the first and the third propellers rotate clockwise and the second and the fourth propellers rotate counterclockwise to generate a positive thrust along the direction of $-\vec{b}_3$, the torque generated by the i -th propeller about \vec{b}_3 can be written as $\tau_i = (-1)^i c_{\tau f} f_i$ for a fixed constant $c_{\tau f}$. All of these assumptions are common [19], [4]. The presented control system can readily be extended to include linear rotor dynamics, as studied in [11].

Under these assumptions, the moment vector in the body-fixed frame is given by

$$M = [d(f_4 - f_2), d(f_1 - f_3), c_{\tau f}(-f_1 + f_2 - f_3 + f_4)].$$

This can be written in matrix form,

$$\begin{bmatrix} f \\ M_1 \\ M_2 \\ M_3 \end{bmatrix} = \begin{bmatrix} 1 & 1 & 1 & 1 \\ 0 & -d & 0 & d \\ d & 0 & -d & 0 \\ -c_{\tau f} & c_{\tau f} & -c_{\tau f} & c_{\tau f} \end{bmatrix} \begin{bmatrix} f_1 \\ f_2 \\ f_3 \\ f_4 \end{bmatrix}. \quad (1)$$

The determinant of the above 4×4 matrix is $8c_{\tau f}d^2$, so it is invertible when $d \neq 0$ and $c_{\tau f} \neq 0$. Therefore, for given thrust magnitude f and given moment vector M , the thrust of each propeller f_1, f_2, f_3, f_4 can be obtained from (1). Using this equation, the thrust magnitude $f \in \mathbb{R}$ and the moment vector $M \in \mathbb{R}^3$ are viewed as control inputs in this paper.

The equations of motion of the quadrotor UAV can be written as

$$\dot{x} = v, \quad (2)$$

$$m\dot{v} = mge_3 - fRe_3, \quad (3)$$

$$\dot{R} = R\hat{\Omega}, \quad (4)$$

$$J\dot{\hat{\Omega}} + \hat{\Omega} \times J\hat{\Omega} = M, \quad (5)$$

where the *hat map* $\hat{\cdot} : \mathbb{R}^3 \rightarrow \mathfrak{so}(3)$ is defined by the condition that $\hat{x}y = x \times y$ for all $x, y \in \mathbb{R}^3$ (see Appendix A).

III. GEOMETRIC TRACKING CONTROL OF A QUADROTOR UAV

Since the quadrotor UAV has four inputs, it is possible to achieve asymptotic output tracking for at most four quadrotor UAV outputs. The quadrotor UAV has three translational and three rotational degrees of freedom; it is not possible to achieve asymptotic output tracking of both attitude and position of the quadrotor UAV. This motivates us to introduce several flight modes. Each flight mode is associated with a specified set of outputs for which exact tracking of those outputs define that flight mode.

The three flight modes considered in this paper are:

- Attitude controlled flight mode: the outputs are the attitude of the quadrotor UAV and the controller for this flight mode achieves asymptotic attitude tracking.

- Position controlled flight mode: the outputs are the position vector of the center of mass of the quadrotor UAV and the controller for this flight mode achieves asymptotic position tracking.
- Velocity controlled flight mode: the outputs are the velocity vector of the center of mass of the quadrotor UAV and the controller for this flight mode achieves asymptotic velocity tracking.

A complex flight maneuver can be defined by specifying a concatenation of flight modes together with conditions for switching between them; for each flight mode one also specifies the desired or commanded outputs as functions of time. For example, one might define a complex aerobatic flight maneuver for the quadrotor UAV that consists of a hovering flight segment by specifying a constant position vector, a reorientation segment by specifying the time evolution of the vehicle attitude, and a surveillance flight segment by specifying a time-varying position vector. The controller in such a case would switch between nonlinear controllers defined for each of the flight modes. These types of complex aerobatic maneuvers, involving large angle transitions between flight modes, have not been much studied in the literature. Such a hybrid flight control architecture has been proposed in [20], [21], [22] for longitudinal flight maneuvers. We use the same hybrid flight control architecture here, although the quadrotor UAV flight model, the flight modes considered, and the nonlinear geometric control approach are different.

IV. ATTITUDE CONTROLLED FLIGHT MODE

We now introduce a nonlinear controller for the attitude controlled flight mode. We show that this controller achieves almost global asymptotic attitude tracking, that is the output attitude of the quadrotor UAV asymptotically tracks the commanded attitude.

An arbitrary smooth attitude tracking command $R_d(t) \in \text{SO}(3)$ is given as a function of time. The corresponding angular velocity command is obtained by the attitude kinematics equation, $\hat{\Omega}_d = R_d^T \dot{R}_d$. We first define errors associated with the attitude dynamics of the quadrotor UAV. The attitude and angular velocity tracking error should be carefully chosen as they evolve on the tangent bundle of $\text{SO}(3)$. First, define the real-valued error function on $\text{SO}(3) \times \text{SO}(3)$:

$$\Psi(R, R_d) = \frac{1}{2} \text{tr}[I - R_d^T R]. \quad (6)$$

This function is locally positive-definite about $R = R_d$ within the region where the rotation angle between R and R_d is less than 180° [14]. For a given R_d , this set can be represented by the sublevel set $L_2 = \{R \in \text{SO}(3) \mid \Psi(R, R_d) < 2\}$, which almost covers $\text{SO}(3)$.

The variation of a rotation matrix can be expressed as $\delta R = R\hat{\eta}$ for $\hat{\eta} \in \mathbb{R}^3$, so that the derivative of the error function is given by

$$\begin{aligned} \mathbf{D}_R \Psi(R, R_d) \cdot R\hat{\eta} &= -\frac{1}{2} \text{tr}[R_d^T R\hat{\eta}] \\ &= \frac{1}{2} (R_d^T R - R^T R_d)^\vee \cdot \hat{\eta}, \end{aligned} \quad (7)$$

where the *vee map* $^\vee : \mathfrak{so}(3) \rightarrow \mathbb{R}^3$ is the inverse of the hat map. We used a property of the hat map given by equation (56) in Appendix A. From this, the attitude tracking error $e_R \in \mathbb{R}^3$ is chosen to be

$$e_R = \frac{1}{2} (R_d^T R - R^T R_d)^\vee. \quad (8)$$

The tangent vectors $\dot{R} \in \mathbb{T}_R \text{SO}(3)$ and $\dot{R}_d \in \mathbb{T}_{R_d} \text{SO}(3)$ cannot be directly compared since they lie in different tangent spaces. We transform \dot{R}_d into a vector in $\mathbb{T}_R \text{SO}(3)$, and we compare it with \dot{R} as follows:

$$\begin{aligned} \dot{R} - \dot{R}_d(R_d^T R) &= R(\hat{\Omega} - R^T R_d \hat{\Omega}_d R_d^T R) \\ &= R(\Omega - R^T R_d \Omega_d)^\wedge, \end{aligned}$$

where we use equation (58) in Appendix A. This motivates our choice of the tracking error for the angular velocity $e_\Omega \in \mathbb{R}^3$ as follows:

$$e_\Omega = \Omega - R^T R_d \Omega_d. \quad (9)$$

We show that e_Ω is the angular velocity vector of the relative rotation matrix $R_d^T R$, represented in the body-fixed frame, since:

$$\begin{aligned} \frac{d}{dt} (R_d^T R) &= -\hat{\Omega}_d R_d^T R + R_d^T R \hat{\Omega} \\ &= R_d^T R (\Omega - R^T R_d \Omega_d)^\wedge = (R_d^T R) \hat{e}_\Omega. \end{aligned} \quad (10)$$

We now introduce a nonlinear controller for the attitude controlled flight mode, described by an expression for the moment vector:

$$\begin{aligned} M &= -k_R e_R - k_\Omega e_\Omega + \Omega \times J\Omega \\ &\quad - J(\hat{\Omega} R^T R_d \Omega_d - R^T R_d \hat{\Omega}_d), \end{aligned} \quad (11)$$

where k_R, k_Ω are positive constants and $R_d(t) \in \text{SO}(3)$ is the specified attitude command for this attitude controlled flight mode. The control moment vector is feedback dependent on the attitude and the angular velocity, and it depends on the commanded attitude, angular velocity and angular acceleration.

In this attitude controlled mode, it is possible to ignore the translational motion of the quadrotor UAV; consequently the reduced model for the attitude dynamics are given by equations (4), (5), using the controller expression (11).

We now state the result that $(e_R, e_\Omega) = (0, 0)$ is an exponentially stable equilibrium of the reduced closed loop dynamics.

Proposition 1: (Exponential Stability of Attitude Controlled Flight Mode) Consider the control moment M defined in (11) for any positive constants k_R, k_Ω . Suppose that the initial conditions satisfy

$$\Psi(R(0), R_d(0)) < 2, \quad (12)$$

$$\|e_\Omega(0)\|^2 < \frac{2}{\lambda_{\max}(J)} k_R (2 - \Psi(R(0), R_d(0))), \quad (13)$$

where $\lambda_{\max}(J)$ denotes the maximum eigenvalue of the inertia matrix J . Then, the zero equilibrium of the closed loop tracking error $(e_R, e_\Omega) = (0, 0)$ is exponentially stable. Furthermore, there exist constants $\alpha_2, \beta_2 > 0$ such that

$$\Psi(R(t), R_d(t)) \leq \min \{2, \alpha_2 e^{-\beta_2 t}\}. \quad (14)$$

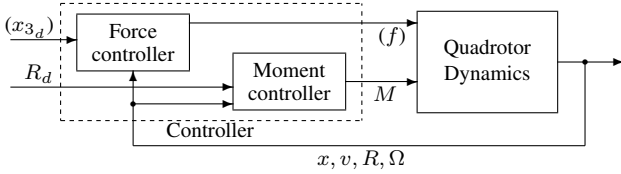


Fig. 2. Controller structure for attitude controlled flight mode (with extensions to altitude tracking)

Proof: See Appendix B. ■

In this proposition, equations (12), (13) describe a region of attraction for the reduced closed loop dynamics. An estimate of the domain of attraction is obtained for which the quadrotor attitude lies in the sublevel set $L_2 = \{R \in \text{SO}(3) \mid \Psi(R, R_d) < 2\}$ for a given R_d . This requires that the initial attitude error should be less than 180° , in terms of the rotation angle about the eigenaxis between R and R_d . Therefore, in Proposition 1, exponential stability is guaranteed for almost all initial attitude errors. More explicitly, the attitudes that lie outside of the region of attraction are of the form $\exp(\pi \hat{s}) R_d$ for some $s \in \mathbb{S}^2$. Since they comprise a two-dimensional manifold in the three-dimensional $\text{SO}(3)$, we claim that the presented controller exhibits *almost global* properties in $\text{SO}(3)$. It should be noted that topological obstructions prevent one from constructing a smooth controller on $\text{SO}(3)$ that has an equilibrium solution that is global asymptotically stable [23]. The size of the region of attraction can be increased by choosing a larger controller gain k_R in (13).

Asymptotic tracking of the quadrotor attitude does not require specification of the thrust magnitude. As an auxiliary problem, the thrust magnitude can be chosen in many different ways to achieve an additional translational motion objective.

As an example of a specific selection approach, we assume that the objective is to asymptotically track a quadrotor altitude command. It is straightforward to obtain the following corollary of Proposition 1.

Proposition 2: (Exponential Stability of Attitude Controlled Flight Mode with Altitude Tracking) Consider the control moment vector M defined in (11) satisfying the assumptions of Proposition 1. In addition, the thrust magnitude is given by

$$f = \frac{k_x(x_3 - x_{3_d}) + k_v(\dot{x}_3 - \dot{x}_{3_d}) + mg - m\ddot{x}_{3_d}}{e_3 \cdot Re_3}, \quad (15)$$

where k_x, k_v are positive constants, $x_{3_d}(t)$ is the quadrotor altitude command, and we assume that

$$e_3 \cdot Re_3 \neq 0. \quad (16)$$

The conclusions of Proposition 1 hold and in addition the quadrotor altitude $x_3(t)$ asymptotically tracks the altitude command $x_{3_d}(t)$.

Proof: See Appendix C. ■

The closed loop system for this flight mode is illustrated in Figure 2. Since the translational motion of the quadrotor UAV can only be partially controlled; this flight mode is most suitable for short time periods where an attitude maneuver

is to be completed. The translational equations of motion of the quadrotor UAV, during an attitude flight mode, are given by equations (2), (3), and whatever thrust magnitude controller, e.g., equation (15), is selected. These equations can be analyzed to determine the full translational motion of the quadrotor UAV during the attitude controlled flight mode.

V. POSITION CONTROLLED FLIGHT MODE

We now introduce a nonlinear controller for the position controlled flight mode. We show that this controller achieves almost global asymptotic position tracking, that is the output position vector of the quadrotor UAV asymptotically tracks the commanded position. This flight mode requires analysis of the coupled translational and rotational equations of motion; hence, we make use of the notation and analysis in the prior section to describe the properties of the closed loop system in this flight mode.

An arbitrary smooth position tracking command $x_d(t) \in \mathbb{R}^3$ is chosen. The position tracking errors for the position and the velocity are given by:

$$e_x = x - x_d, \quad (17)$$

$$e_v = v - \dot{x}_d. \quad (18)$$

The nonlinear controller for the position controlled flight mode, described by control expressions for the thrust magnitude and the moment vector, are:

$$f = (k_x e_x + k_v e_v + m g e_3 - m \ddot{x}_d) \cdot R e_3, \quad (19)$$

$$M = -k_R e_R - k_\Omega e_\Omega + \Omega \times J \Omega - J(\hat{\Omega} R^T R_c \Omega_c - R^T R_c \hat{\Omega}_c), \quad (20)$$

where k_x, k_v, k_R, k_Ω are positive constants. Following the prior definition of the attitude error and the angular velocity error

$$e_R = \frac{1}{2}(R_c^T R - R^T R_c)^\vee, \quad e_\Omega = \Omega - R^T R_c \Omega_c, \quad (21)$$

and the computed attitude $R_c(t) \in \text{SO}(3)$ and computed angular velocity $\Omega_c \in \mathbb{R}^3$ are given by

$$R_c = [b_{1c}; b_{3c} \times b_{1c}; b_{3c}], \quad \hat{\Omega}_c = R_c^T \dot{R}_c, \quad (22)$$

where $b_{3c} \in \mathbb{S}^2$ is defined by

$$b_{3c} = -\frac{-k_x e_x - k_v e_v - m g e_3 + m \ddot{x}_d}{\| -k_x e_x - k_v e_v - m g e_3 + m \ddot{x}_d \|}, \quad (23)$$

and $b_{1c} \in \mathbb{S}^2$ is selected to be orthogonal to b_{3c} , thereby guaranteeing that $R_c \in \text{SO}(3)$. We assume that

$$\| -k_x e_x - k_v e_v - m g e_3 + m \ddot{x}_d \| \neq 0, \quad (24)$$

and the commanded acceleration is uniformly bounded such that

$$\| -m g e_3 + m \ddot{x}_d \| < B \quad (25)$$

for a given positive constant B .

The thrust magnitude controller and the moment vector controller is feedback dependent on the position and translational velocity and they depend on the commanded position,

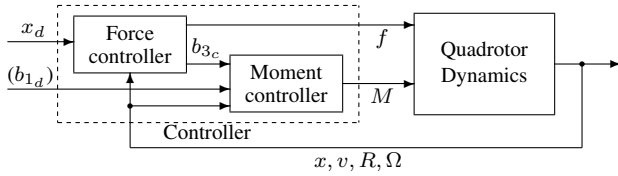


Fig. 3. Controller structure for position controlled flight mode

translational velocity and translational acceleration. The control moment vector has a form that is similar to that for the attitude controlled flight mode. However, the *attitude error* and *angular velocity error* are defined with respect to a computed attitude, angular velocity and angular acceleration, that are constructed according to the indicated procedure.

The nonlinear controller given by equations (19), (20) can be given a backstepping interpretation. The computed attitude R_c given in equation (22) is selected so that the thrust axis $-b_3$ of the quadrotor UAV tracks the computed direction given by $-b_{3_c}$ in (23), which is a direction of the thrust vector that achieves position tracking. The moment expression (20) causes the attitude of the quadrotor UAV to asymptotically track R_c and the thrust magnitude expression (19) achieves asymptotic position tracking.

The closed loop system for this position controlled flight mode is illustrated in Figure 3. The corresponding closed loop control system is described by equations (2), (3), (4), (5), using the controller expressions (19) and (20).

We now state the result that $(e_x, e_v, e_R, e_\Omega) = (0, 0, 0, 0)$ is an exponentially stable equilibrium of the closed loop dynamics.

Proposition 3: (Exponential Stability of Position Controlled Flight Mode) Consider the thrust magnitude f and moment vector M defined by equations (19), (20). Suppose that the initial conditions satisfy

$$\Psi(R(0), R_c(0)) < 1. \quad (26)$$

Define $W_1, W_{12}, W_2 \in \mathbb{R}^{2 \times 2}$ to be

$$W_1 = \begin{bmatrix} \frac{c_1 k_x}{m} & -\frac{c_1 k_v}{2m}(1 + \alpha) \\ -\frac{c_1 k_v}{2m}(1 + \alpha) & k_v(1 - \alpha) - c_1 \end{bmatrix}, \quad (27)$$

$$W_{12} = \begin{bmatrix} k_x e_{v_{\max}} + \frac{c_1}{m} B & 0 \\ B & 0 \end{bmatrix}, \quad (28)$$

$$W_2 = \begin{bmatrix} \frac{c_2 k_R}{\lambda_{\max}(J)} & -\frac{c_2 k_\Omega}{2\lambda_{\min}(J)} \\ -\frac{c_2 k_\Omega}{2\lambda_{\min}(J)} & k_\Omega - c_2 \end{bmatrix}, \quad (29)$$

where $\Psi(R(0), R_c(0)) < \psi_1 < 1$, $\alpha = \sqrt{\psi_1(2 - \psi_1)}$, $e_{v_{\max}} = \max\{\|e_v(0)\|, \frac{B}{k_v(1 - \alpha)}\}$. For positive constants k_x, k_v , we choose positive constants c_1, c_2, k_R, k_Ω such that

$$c_1 < \min \left\{ k_v(1 - \alpha), \frac{4mk_x k_v(1 - \alpha)}{k_v^2(1 + \alpha)^2 + 4mk_x}, \sqrt{k_x m} \right\}, \quad (30)$$

$$c_2 < \min \left\{ k_\Omega, \frac{4k_\Omega k_R \lambda_{\min}(J)^2}{k_\Omega^2 \lambda_{\max}(J) + 4k_R \lambda_{\min}(J)^2}, \sqrt{k_R \lambda_{\min}(J)} \right\}, \quad (31)$$

$$\lambda_{\min}(W_2) > \frac{4\|W_{12}\|^2}{\lambda_{\min}(W_1)}. \quad (32)$$

Then, the zero equilibrium of the closed loop tracking errors $(e_x, e_v, e_R, e_\Omega) = (0, 0, 0, 0)$ is exponentially stable. A region of attraction is characterized by (26) and

$$\|e_\Omega(0)\|^2 < \frac{2}{\lambda_{\max}(J)} k_R (\psi_1 - \Psi(R(0), R_c(0))). \quad (33)$$

Proof: See Appendix D. ■

Proposition 3 requires that the initial *attitude error* is less than 90° to achieve exponential stability for this flight mode. Suppose that this is not satisfied, i.e. $1 \leq \Psi(R(0), R_c(0)) < 2$. We can apply Proposition 1, which states that the attitude error function Ψ exponentially decreases, and therefore, it enters the region of attraction of Proposition 3 in a finite time. Therefore, by combining the results of Proposition 1 and 3, we can show almost global exponential attractiveness when $\Psi(R(0), R_c(0)) < 2$.

Definition 1: (Exponential Attractiveness [24]) An equilibrium point $z = 0$ of a dynamic system is *exponentially attractive* if, for some $\delta > 0$, there exists a constant $\alpha(\delta) > 0$ and $\beta > 0$ such that $\|z(0)\| < \delta$ implies $\|z(t)\| \leq \alpha(\delta)e^{-\beta t}$ for all $t > 0$.

This should be distinguished from the stronger notion of exponential stability, in which the above bound is replaced by $\|z(t)\| \leq \alpha(\delta)\|z(0)\|e^{-\beta t}$.

Proposition 4: (Almost Global Exponential Attractiveness of the Position Controlled Flight Mode) Consider the thrust magnitude f and moment vector M defined in expressions (19), (20). Suppose that the initial conditions satisfy

$$1 \leq \Psi(R(0), R_c(0)) < 2, \quad (34)$$

$$\|e_\Omega(0)\|^2 < \frac{2}{\lambda_{\max}(J)} k_R (2 - \Psi(R(0), R_c(0))). \quad (35)$$

Then, the zero equilibrium of the closed loop tracking errors $(e_x, e_v, e_R, e_\Omega) = (0, 0, 0, 0)$ is exponentially attractive.

Proof: See Appendix E. ■

In Proposition 4, exponential attractiveness is guaranteed for almost all initial attitude errors. Since the attitudes that lie outside of the region of attraction comprise a two-dimensional manifold in the three-dimensional $SO(3)$, as discussed in Section IV, we claim that the presented controller exhibits *almost global* properties in $SO(3)$.

Note that the *attitude error* defined above is based on the computed attitude $R_c \in SO(3)$, which is feedback dependent in the manner specified above. Note that the construction of R_c is not completely determined. The construction of the orthogonal matrix R_c involves having its third column b_{3_c} specified by a normalized feedback function, and its first column b_{1_c} is chosen to be orthogonal to the third column. The unit vector b_{1_c} can be arbitrarily chosen in the plane normal to b_{3_c} , which corresponds to a one-dimensional degree of choice. This reflects the fact that the quadrotor UAV has four control inputs that are used to track a three-dimensional position command.

By choosing b_{1_c} properly, we constrain the asymptotic direction of the first body-fixed axis. Here, we propose to specify the *projection* of the first body-fixed axis onto the plane normal to b_{3_c} . In particular, we choose a desired direction $b_{1_d} \in S^2$, that is not parallel to b_{3_c} , and b_{1_c} is selected

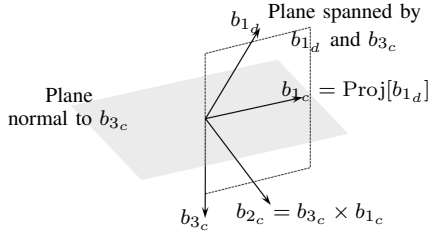


Fig. 4. Convergence property of the first body-fixed axis: b_{3c} is determined by (23). We choose an arbitrary b_{1d} that is not parallel to b_{3c} , and project it on to the plane normal to b_{3c} to obtain b_{1c} . This guarantees that the first body-fixed axis asymptotically lies in the plane spanned by b_{1d} and b_{3c} , which converges to the direction of $ge_3 - \ddot{x}_d$ as $t \rightarrow \infty$.

as $b_{1c} = \text{Proj}[b_{1d}]$, where $\text{Proj}[\cdot]$ denotes the normalized projection onto the plane perpendicular to b_{3c} . In this case, the first body-fixed axis does not converge to b_{1d} , but it converges to the projection of b_{1d} , i.e. $b_1 \rightarrow b_{1c} = \text{Proj}[b_{1d}]$ as $t \rightarrow \infty$. In other words, the first body-fixed axis converges to the intersection of the plane normal to b_{3c} and the plane spanned by b_{3c} and b_{1d} (see Figure 4). From (23), we observe that b_{3c} asymptotically converges to the direction $ge_3 - \ddot{x}_d$. In short, the additional input is used to guarantee that the first body-fixed axis asymptotically lies in the plane spanned by b_{1d} and $ge_3 - \ddot{x}_d$.

Suppose that $\ddot{x}_d = 0$, then the third body-fixed axis converges to the gravity direction e_3 . In this case, we can choose b_{1d} arbitrarily in the horizontal plane, and it follows that $b_{1c} \rightarrow \text{Proj}[b_{1d}] = b_{1d}$ as $t \rightarrow \infty$. Therefore, the first body-fixed axis b_1 asymptotically converges to b_{1d} , which can be used to specify the heading direction of the quadrotor UAV in the horizontal plane. These arguments are summarized as follows.

Proposition 5: (Almost Global Exponential Attractiveness of Position Controlled Flight Mode with Specified Asymptotic Direction of First Body-Fixed Axis) Consider the moment vector M defined in (20) and the thrust magnitude f defined in (19) satisfying the assumptions of Propositions 3 and 4.

In addition, the first column of R_c , namely b_{1c} is constructed as follows. We choose $b_{1d}(t) \in S^2$, and we assume that it is not parallel to b_{3c} . The unit vector b_{1c} is constructed by projecting b_{1d} onto the plane normal to b_{3c} , and normalizing it:

$$b_{1c} = -\frac{1}{\|b_{3c} \times b_{1d}\|} (b_{3c} \times (b_{3c} \times b_{1d})). \quad (36)$$

Then, the conclusions of Propositions 3 and 4 hold, and the first body-fixed axis asymptotically lies in the plane spanned by b_{1d} and $ge_3 - \ddot{x}_d$.

In the special case where $\ddot{x}_d = 0$, we can choose b_{1d} in the horizontal plane. Then, the first body-fixed axis asymptotically converges to b_{1d} .

Expressions for Ω_c and $\dot{\Omega}_c$ that appear in Proposition 5 are summarized in [25]. These additional properties of the closed loop can be interpreted as characterizing the asymptotic direction of the first body-fixed axis and the asymptotic direction of the third body-fixed axis as it depends on the commanded vehicle acceleration. These physical properties may be of importance in some flight maneuvers.

VI. VELOCITY CONTROLLED FLIGHT MODE

We now introduce a nonlinear controller for the velocity controlled flight mode. We show that this controller achieves almost global asymptotic velocity tracking, that is the output velocity vector of the quadrotor UAV asymptotically tracks the commanded velocity.

An arbitrary smooth velocity tracking command $v_d(t) \in \mathbb{R}^3$ is given. The velocity tracking error given by:

$$e_v = v - v_d. \quad (37)$$

The nonlinear controller for the velocity controlled flight mode, described by control expressions for the thrust magnitude and the moment vector, are:

$$f = (k_v e_v + mge_3 - m\dot{v}_d) \cdot Re_3, \quad (38)$$

$$M = -k_R e_R - k_\Omega e_\Omega + \Omega \times J\Omega - J(\hat{\Omega}R^T R_c \Omega_c - R^T R_c \dot{\Omega}_c), \quad (39)$$

where k_v, k_R, k_Ω are positive constants, and following the prior definitions

$$e_R = \frac{1}{2}(R_c^T R - R^T R_c)^\vee, \quad e_\Omega = \Omega - R^T R_c \Omega_c, \quad (40)$$

and the control attitude $R_c(t) \in \text{SO}(3)$ and control angular velocity $\Omega_c \in \mathbb{R}^3$ are given by

$$R_c = [b_{1c}; b_{3c} \times b_{1c}; b_{3c}], \quad \hat{\Omega}_c = R_c^T \dot{R}_c, \quad (41)$$

where $b_{3c} \in S^2$ is defined by

$$b_{3c} = -\frac{-k_v e_v - mge_3 + m\dot{v}_d}{\|-k_v e_v - mge_3 + m\dot{v}_d\|}, \quad (42)$$

and $b_{1c} \in S^2$ is selected to be orthogonal to b_{3c} , thereby guaranteeing that $R_c(t) \in \text{SO}(3)$. We assume that

$$\|-k_v e_v - mge_3 + m\dot{v}_d\| \neq 0, \quad (43)$$

and the commanded acceleration is uniformly bounded

$$\|-mge_3 + m\dot{v}_d\| < B \quad (44)$$

for a given positive constant B .

The overall controller structure is similar to the position controlled flight mode. Since only v_d is specified, the position error e_x in (23) is zero, and \ddot{x}_d is replaced by \dot{v}_d in (42). The control thrust magnitude and the control moment vector is feedback dependent on the translational velocity and they depend on the commanded translational velocity and translational acceleration. The control moment vector has a form that is similar to that for the attitude controlled flight mode. However, the *attitude error* and *angular velocity error* are defined with respect to a computed attitude, angular velocity and angular acceleration, that are constructed according to the indicated procedure. This construction has the property that the direction of the thrust vector, namely $-Re_3$, is such that the thrust magnitude (38) achieves the desired velocity tracking objectives.

We now state the result that $(e_v, e_R, e_\Omega) = (0, 0, 0)$ is an exponentially stable equilibrium of the closed loop dynamics.

Proposition 6: (Exponential Stability of Velocity Controlled Flight Mode) Consider the thrust magnitude f and

moment vector M defined by equations (38), (39). Suppose that the initial conditions satisfy

$$\Psi(R(0), R_c(0)) < 1. \quad (45)$$

Define $W_2 \in \mathbb{R}^{2 \times 2}$ to be

$$W_2 = \begin{bmatrix} \frac{c_2 k_R}{\lambda_{\max}(J)} & -\frac{c_2 k_\Omega}{2\lambda_{\min}(J)} \\ -\frac{c_2 k_\Omega}{2\lambda_{\min}(J)} & k_\Omega - c_2 \end{bmatrix}, \quad (46)$$

For positive constants k_v , we choose positive constants c_2, k_R, k_Ω such that

$$c_2 < \min \left\{ k_\Omega, \frac{4k_\Omega k_R \lambda_{\min}(J)^2}{k_\Omega^2 \lambda_{\max}(J) + 4k_R \lambda_{\min}(J)^2}, \sqrt{k_R \lambda_{\min}(J)} \right\}, \quad (47)$$

$$\lambda_{\min}(W_2) > \frac{4B^2}{k_v(1-\alpha)}, \quad (48)$$

where $\Psi(R(0), R_c(0)) < \psi_1 < 1$, $\alpha = \sqrt{\psi_1(2-\psi_1)}$. Then, the zero equilibrium of the closed loop tracking errors $(e_v, e_R, e_\Omega) = (0, 0, 0)$ is exponentially stable. A region of attraction is characterized by (45) and

$$\|e_\Omega(0)\|^2 < \frac{2}{\lambda_{\max}(J)} k_R (\psi_1 - \Psi(R(0), R_c(0))). \quad (49)$$

Proposition 6 requires that the initial *attitude error* is less than 90° to achieve exponential stability for this flight mode. Similar to Proposition 4, we can show almost global exponential attractiveness when $\Psi(R(0), R_c(0)) < 2$.

Proposition 7: (Almost Global Exponential Attractiveness of Velocity Controlled Flight Mode) Consider the thrust magnitude f and moment vector M defined in expressions (38), (39). Suppose that the initial conditions satisfy

$$1 \leq \Psi(R(0), R_c(0)) < 2, \quad (50)$$

$$\|e_\Omega(0)\|^2 < \frac{2}{\lambda_{\max}(J)} k_R (2 - \Psi(R(0), R_c(0))). \quad (51)$$

Then, the zero equilibrium of the closed loop tracking errors $(e_v, e_R, e_\Omega) = (0, 0, 0)$ is exponentially attractive.

The proofs for Propositions 6 and 7 are similar to Propositions 3 and 4, respectively, and they are relegated to [25]. As described in Section V, there is freedom in constructing $R_c \in \text{SO}(3)$. This freedom can be used as discussed in Proposition 5.

Proposition 8: (Almost Global Exponential Attractiveness of Velocity Controlled Flight Mode with Specified Asymptotic Direction of First Body-Fixed Axis) Consider the moment vector M defined in (39) and the thrust magnitude f defined in (38) satisfying the assumptions of Propositions 6 and 7.

In addition, the first column of R_c , namely b_{1_c} is constructed as follows. We choose $b_{1_d}(t) \in \mathbb{S}^2$, and we assume that it is not parallel to b_{3_c} . The unit vector b_{1_c} is constructed by projecting b_{1_d} onto the plane normal to b_{3_c} , and normalizing it:

$$b_{1_c} = -\frac{1}{\|b_{3_c} \times b_{1_d}\|} (b_{3_c} \times (b_{3_c} \times b_{1_d})). \quad (52)$$

Then, the conclusions of Propositions 6 and 7 hold, and the first body-fixed axis asymptotically lies in the plane spanned by b_{1_d} and $ge_3 - \dot{v}_d$.

In the special case where $\dot{v}_d = 0$, we can choose b_{1_d} to lie in the horizontal plane. Then, the first body-fixed axis asymptotically converges to b_{1_d} .

VII. NUMERICAL RESULTS ILLUSTRATING COMPLEX FLIGHT MANEUVERS

Numerical results are presented to demonstrate the prior approach for performing complex flight maneuvers for a typical quadrotor UAV. The parameters are chosen to match a quadrotor UAV described in [2].

$$J = [0.0820, 0.0845, 0.1377] \text{ kg} \cdot \text{m}^2, \quad m = 4.34 \text{ kg} \\ d = 0.315 \text{ m}, \quad c_{\tau f} = 8.004 \times 10^{-3} \text{ m}.$$

The controller parameters are chosen as follows:

$$k_x = 16m, \quad k_v = 5.6m, \quad k_R = 8.81, \quad k_\Omega = 2.54.$$

We consider two complex flight maneuvers. The first case corresponds to the position controlled mode; the results in Proposition 4 are referenced. The second case involves transitions between all of the three flight modes.

Case (I): Position Controlled Flight Mode: Consider a hovering maneuver for which the quadrotor UAV recovers from being initially upside down. The desired tracking commands are as follows.

$$x_d(t) = [0, 0, 0], \quad b_{1_d}(t) = [1, 0, 0].$$

and it is desired to maintain the quadrotor UAV at a constant altitude. Initial conditions are chosen as

$$x(0) = [0, 0, 0], \quad v(0) = [0, 0, 0], \\ R(0) = \begin{bmatrix} 1 & 0 & 0 \\ 0 & -0.9995 & -0.0314 \\ 0 & 0.0314 & -0.9995 \end{bmatrix}, \quad \Omega(0) = [0, 0, 0].$$

This initial condition corresponds to an upside down quadrotor UAV.

The preferred direction of the total thrust vector in the controlled system is $-b_3$. But initially, it is given by $-b_3(0) = -R(0)e_3 = [0, 0.0314, 0.9995]$, which is almost opposite to the thrust direction $[0, 0, -1]$ required for the given hovering command. This yields a large initial attitude error, namely 178° in terms of the rotation angle about the eigen-axis between $R_c(0)$ and $R(0)$, and the corresponding the initial *attitude error* is $\Psi(0) = 1.995$.

Therefore, we cannot apply Proposition 3 that gives exponential stability when $\Psi(0) < 1$, but by Proposition 4, we can guarantee exponential attractiveness. From Proposition 1, the *attitude error* function Ψ decreases; it eventually becomes less than 1 at $t = 0.88$ seconds as illustrated in Figure 5(a). At that instant, the *attitude error* enters the region of attraction specified in Proposition 3. Therefore, for $t > 0.88$ seconds, the position tracking error converges to zero exponentially as shown in Figures 5(b). The region of attraction of the proposed control system almost covers $\text{SO}(3)$, so that the controlled quadrotor UAV can recover from being initially upside down.

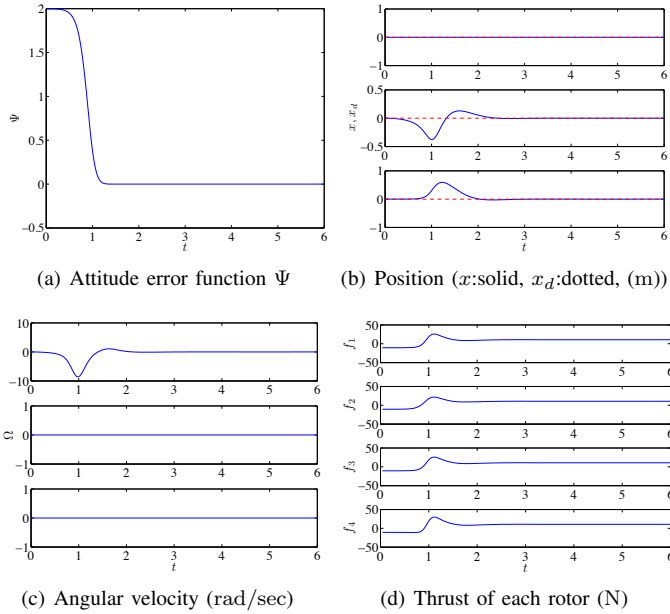


Fig. 5. Case I: position controlled flight mode for a hovering, recovering from an initially upside down attitude

Case (II): Transition Between Several Flight Modes: This flight maneuver consists of a sequence of five flight modes, including a rotation by 720° (see Figure 6).

(a) Velocity controlled flight mode ($t \in [0, 4)$)

$$v_d(t) = [1 + 0.5t, 0.2 \sin(2\pi t), -0.1], \quad b_{1_d}(t) = [1, 0, 0].$$

(b) Attitude controlled flight mode ($t \in [4, 6)$): rotation about the second body-fixed axis by 720°

$$R_d(t) = \exp(2\pi(t-4)\hat{e}_2).$$

(c) Position controlled flight mode ($t \in [6, 8)$)

$$x_d(t) = [14 - t, 0, 0], \quad b_{1_d}(t) = [1, 0, 0].$$

(d) Attitude controlled flight mode ($t \in [8, 9)$): rotation about the first body-fixed axis by 360°

$$R_d(t) = \exp(2\pi(t-8)\hat{e}_1).$$

(e) Position controlled flight mode ($t \in [9, 12]$)

$$x_d(t) = [20 - \frac{5}{3}t, 0, 0], \quad b_{1_d}(t) = [0, 1, 0].$$

Initial conditions are same as the first case.

The second case involves transitions between several flight modes. It begins with a velocity controlled flight mode. As the initial attitude error function is less than 1, according to Proposition 6, the velocity tracking error exponentially converges as shown at Figure 7(d). From Proposition 8, the first body-fixed axis asymptotically lies in the plane spanned by $b_{1_d} = e_1$ and $ge_3 - \dot{v}_d$. Since $\|\dot{v}_d\| \ll g$, the first body-fixed axis remains close to the plane composed of e_1 and e_3 , as illustrated in Figure 7(e).

This is followed by an attitude tracking mode to rotate the quadrotor by 720° about the second body-fixed axis according to Proposition 1. As discussed in Section IV, the thrust

magnitude f can be arbitrarily chosen in an attitude controlled flight mode. We cannot apply the results of Proposition 2 for altitude tracking, since the third body-fixed axis becomes horizontal several times during the given attitude maneuver. Here we choose the thrust magnitude given by

$$f(t) = (k_x(x(t) - x_c) + k_v v(t) + mge_3) \cdot R(t)e_3,$$

which is equivalent to the thrust magnitude for the position controlled flight mode given in (19), when $x_d(t) = x_c = [8, 0, 0]$. This does not guarantee asymptotic convergence of the quadrotor UAV position to $[8, 0, 0]$ since the direction of the total thrust is determined by the given attitude command. But, it has the effects that the position of the quadrotor UAV stays close to x_c , as illustrated at Figure 7(b).

Next, a position tracking mode is again engaged, and the quadrotor UAV soon follows a straight line. Another attitude tracking mode and a position tracking mode are repeated to rotate the quadrotor by 360° about the direction of the second body-fixed axis. The thrust magnitude is chosen as

$$f(t) = (k_x(x(t) - x_c) + k_v v(t) + mge_3) \cdot R(t)e_3,$$

where $x_c = [6, 0, 0]$, to make the position of the quadrotor UAV remain close to x_c during this attitude maneuver, as discussed above. For the position tracking modes (c) and (e), we have $\dot{x}_d = 0$, and b_{1_d} lies in the horizontal plane. Therefore, according to Proposition 5, the first body-fixed b_1 asymptotically converges to b_{1_d} , as shown at Figure 7(e). For example, during the last position tracking mode (e), the first body-fixed axis points to the left of the flight path since b_{1_d} is specified to be e_2 . These illustrate that by switching between an attitude mode and a position and heading flight mode, the quadrotor UAV can perform the prescribed complex acrobatic maneuver.

VIII. CONCLUSIONS

We presented a global dynamic model for a quadrotor UAV, and we developed tracking controllers for three different flight modes; these were developed in terms of the special Euclidean group that is intrinsic and coordinate-free, thereby avoiding the singularities of Euler angles and the ambiguities of quaternions in representing attitude. Using the proposed geometric based controllers for the three flight modes we studied, the quadrotor exhibits exponential stability when the initial attitude error is less than 90° , and it yields almost global exponential attractiveness when the initial attitude error is less than 180° . By switching between different controllers for these flight modes, we have demonstrated that the quadrotor UAV can perform complex acrobatic maneuvers. Several different complex flight maneuvers were demonstrated in the numerical examples.

APPENDIX

A. Properties of the Hat Map

The hat map $\hat{\cdot} : \mathbb{R}^3 \rightarrow \mathfrak{so}(3)$ is defined as

$$\hat{x} = \begin{bmatrix} 0 & -x_3 & x_2 \\ x_3 & 0 & -x_1 \\ -x_2 & x_1 & 0 \end{bmatrix} \quad (53)$$

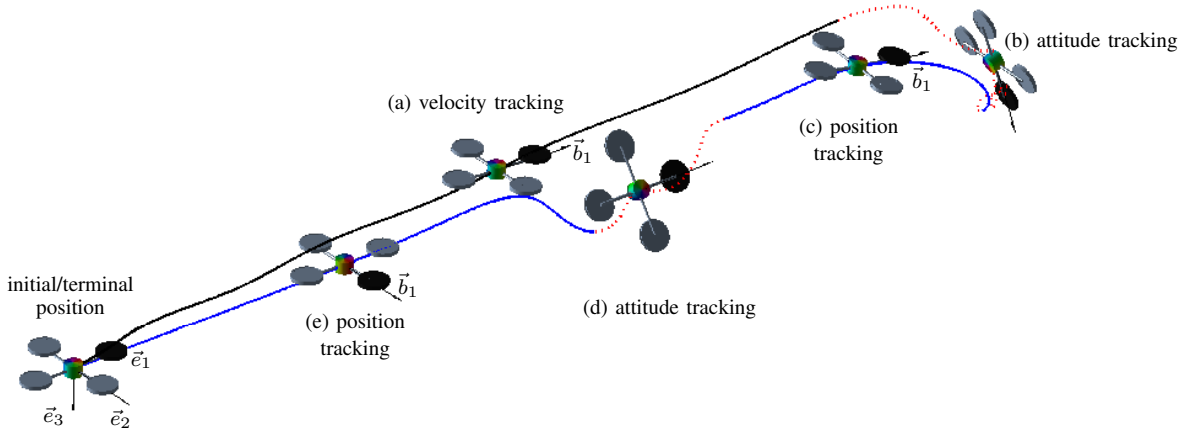


Fig. 6. Case II: complex maneuver of a quadrotor UAV involving a rotation by 720° about \bar{e}_2 (b), and a rotation by 360° about \bar{e}_1 (d), with transitions between several flight modes. The direction of the first body-fixed axis is specified for velocity/position tracking modes ((a),(c),(e)) (an animation illustrating this maneuver is available at <http://my.fit.edu/~taeyoung>).

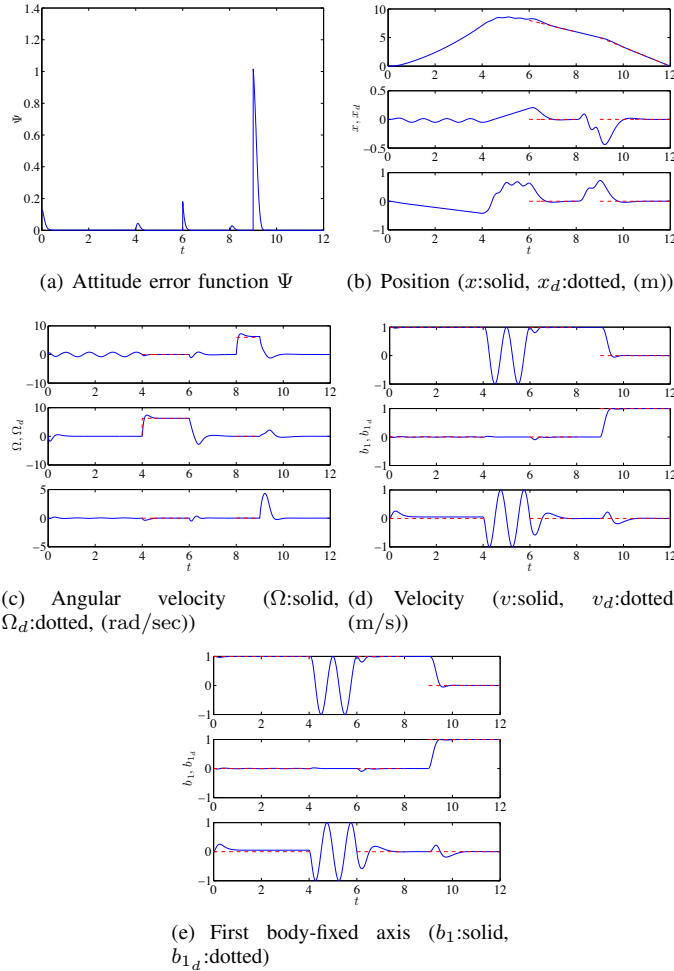


Fig. 7. Case II: transitions between several flight modes for a complex maneuver

for $x = [x_1; x_2; x_3] \in \mathbb{R}^3$. This identifies the Lie algebra $\mathfrak{so}(3)$ with \mathbb{R}^3 using the vector cross product in \mathbb{R}^3 . The inverse of the hat map is referred to as the *vee* map, $\vee : \mathfrak{so}(3) \rightarrow \mathbb{R}^3$. Several properties of the hat map are summarized as follows.

$$\hat{x}y = x \times y = -y \times x = -\hat{y}x, \quad (54)$$

$$-\frac{1}{2}\text{tr}[\hat{x}\hat{y}] = x^T y, \quad (55)$$

$$\text{tr}[\hat{x}A] = \text{tr}[A\hat{x}] = \frac{1}{2}\text{tr}[\hat{x}(A - A^T)] = -x^T(A - A^T)\vee, \quad (56)$$

$$\hat{x}A + A^T\hat{x} = (\{\text{tr}[A]I_{3 \times 3} - A\}x)^\wedge, \quad (57)$$

$$R\hat{x}R^T = (Rx)^\wedge, \quad (58)$$

for any $x, y \in \mathbb{R}^3$, $A \in \mathbb{R}^{3 \times 3}$, and $R \in \text{SO}(3)$.

B. Proof of Proposition 1

We first find the error dynamics for e_R, e_Ω , and define a Lyapunov function. Then, we show that under the given conditions, $R(t)$ always lies in the sublevel set L_2 , which guarantees the positive-definiteness of the attitude error function Ψ . From this, we show exponential stability of the attitude error dynamics.

a) Attitude Error Dynamics: We find the error dynamics for Ψ, e_R, e_Ω as follows. Using the attitude kinematics equations, namely $\dot{R} = R\hat{\Omega}$, $\dot{R}_d = R_d\hat{\Omega}_d$, and equations (9), (58), the time derivative of Ψ is given by

$$\begin{aligned} \dot{\Psi}(R, R_d) &= -\frac{1}{2}\text{tr}\left[-\hat{\Omega}_d R_d^T R + R_d^T R \hat{\Omega}\right] \\ &= -\frac{1}{2}\text{tr}\left[R_d^T R(\hat{\Omega} - R^T R_d \hat{\Omega}_d R_d^T R)\right] = -\frac{1}{2}\text{tr}\left[R_d^T R \hat{e}_\Omega\right]. \end{aligned}$$

By (56), this can be written as

$$\dot{\Psi}(R, R_d) = \frac{1}{2}e_\Omega^T (R_d^T R - R^T R_d)^\vee = e_R \cdot e_\Omega. \quad (59)$$

Using equations (10) and (57), the time derivative of e_R can be written as

$$\begin{aligned} \dot{e}_R &= \frac{1}{2}(R_d^T R \hat{e}_\Omega + \hat{e}_\Omega R^T R_d)^\vee \\ &= \frac{1}{2}(\text{tr}[R^T R_d]I - R^T R_d)e_\Omega \equiv C(R_d^T R)e_\Omega. \end{aligned} \quad (60)$$

Now we show that $\|C(R_d^T R)\|_2 \leq 1$ for any $R_d^T R \in \text{SO}(3)$. Using Rodrigues' formula [14], we can show that the eigenvalues of $C^T(\exp \hat{x})C(\exp \hat{x})$ are given by $\cos^2 \|x\|$, $\frac{1}{2}(1 + \cos \|x\|)$, and $\frac{1}{2}(1 - \cos \|x\|)$, which are less than or equal to 1 for any $x \in \mathbb{R}^3$. Therefore, $\|C(R_d^T R)\|_2 \leq 1$, and this implies that

$$\|\dot{e}_R\| \leq \|e_\Omega\|. \quad (61)$$

From equation (9), the time derivative of e_Ω is given by

$$J\dot{e}_\Omega = J\dot{\Omega} + J(\hat{\Omega}R^T R_d \Omega_d - R^T R_d \hat{\Omega}_d),$$

where we use a property of the hat map, $\hat{x}x = 0$ for any $x \in \mathbb{R}^3$. Substituting the equation of motion (5) and the control moment (20), this reduces to

$$J\dot{e}_\Omega = -k_R e_R - k_\Omega e_\Omega. \quad (62)$$

In short, the attitude error dynamics are given by equations (59), (60), (62), and they satisfy (61).

b) Lyapunov Candidate: For a non-negative constant c_2 , let a Lyapunov candidate \mathcal{V}_2 be

$$\mathcal{V}_2 = \frac{1}{2}e_\Omega \cdot J e_\Omega + k_R \Psi(R, R_d) + c_2 e_R \cdot e_\Omega. \quad (63)$$

From equations (59), (60), (62), the time derivative of \mathcal{V}_2 is given by

$$\begin{aligned} \dot{\mathcal{V}}_2 &= e_\Omega \cdot J\dot{e}_\Omega + k_R e_R \cdot e_\Omega + c_2 \dot{e}_R \cdot e_\Omega + c_2 e_R \cdot \dot{e}_\Omega \\ &= -k_\Omega \|e_\Omega\|^2 - c_2 k_R e_R \cdot J^{-1} e_R + c_2 C(R_d^T R) e_\Omega \cdot e_\Omega \\ &\quad - c_2 k_\Omega e_R \cdot J^{-1} e_\Omega. \end{aligned} \quad (64)$$

Since $\|C(R_d^T R)\| \leq 1$, this is bounded by

$$\begin{aligned} \dot{\mathcal{V}}_2 &\leq -(k_\Omega - c_2) \|e_\Omega\|^2 - \frac{c_2 k_R}{\lambda_{\max}(J)} \|e_R\|^2 + \frac{c_2 k_\Omega}{\lambda_{\min}(J)} \|e_R\| \|e_\Omega\| \\ &= -z_2^T W_2 z_2, \end{aligned} \quad (65)$$

where $z_2 = [\|e_R\|, \|e_\Omega\|]^T$, and the matrix $W_2 \in \mathbb{R}^{2 \times 2}$ is given by

$$W_2 = \begin{bmatrix} \frac{c_2 k_R}{\lambda_{\max}(J)} & -\frac{c_2 k_\Omega}{2\lambda_{\min}(J)} \\ -\frac{c_2 k_\Omega}{2\lambda_{\min}(J)} & k_\Omega - c_2 \end{bmatrix}. \quad (66)$$

c) Boundedness of Ψ : Define $\mathcal{V}'_2 = \mathcal{V}_2|_{c_2=0}$. From (63), (64), we have

$$\begin{aligned} \mathcal{V}'_2 &= \frac{1}{2}e_\Omega \cdot J e_\Omega + k_R \Psi(R, R_d), \\ \dot{\mathcal{V}}'_2 &= -k_\Omega \|e_\Omega\|^2 \leq 0. \end{aligned}$$

This implies that \mathcal{V}'_2 is non-increasing, i.e., $\mathcal{V}'_2(t) \leq \mathcal{V}'_2(0)$. Using (13), the initial value of \mathcal{V}'_2 is bounded by $\mathcal{V}'_2(0) < 2k_R$. Therefore, we obtain

$$k_R \Psi(R(t), R_d(t)) \leq \mathcal{V}'_2(t) \leq \mathcal{V}'_2(0) < 2k_R. \quad (67)$$

Therefore, the attitude error function is bounded by

$$\Psi(R(t), R_d(t)) \leq \psi_2 < 2, \quad \text{for any } t \geq 0, \quad (68)$$

and for $\psi_2 = \frac{1}{k_R} \mathcal{V}'_2(0)$. Therefore, $R(t)$ always lies in the sublevel set $L_2 = \{R \in \text{SO}(3) \mid \Psi(R, R_d) < 2\}$.

d) Exponential Stability: Now, we show exponential stability of the attitude dynamics by considering the general case where the constant c_2 is positive. Using Rodrigues' formula, we can show that

$$\Psi(R, R_d) = 1 - \cos \|x\|, \quad (69)$$

$$\begin{aligned} \|e_R\|^2 &= \sin^2 \|x\| = (1 + \cos \|x\|)\Psi(R, R_d) \\ &= (2 - \Psi(R, R_d))\Psi(R, R_d), \end{aligned} \quad (70)$$

when $R_d^T R = \exp \hat{x}$ for $x \in \mathbb{R}^3$. Therefore, from (68), the attitude error function satisfies

$$\frac{1}{2} \|e_R\|^2 \leq \Psi(R, R_d) \leq \frac{1}{2 - \psi_2} \|e_R\|^2. \quad (71)$$

This implies that Ψ is positive-definite and decrescent. It follows that the Lyapunov function \mathcal{V}_2 is bounded as

$$z_2^T M_{21} z_2 \leq \mathcal{V}_2 \leq z_2^T M_{22} z_2, \quad (72)$$

where

$$M_{21} = \frac{1}{2} \begin{bmatrix} k_R & -c_2 \\ -c_2 & \lambda_{\min}(J) \end{bmatrix}, \quad M_{22} = \frac{1}{2} \begin{bmatrix} \frac{2k_R}{2-\psi_2} & c_2 \\ c_2 & \lambda_{\max}(J) \end{bmatrix}. \quad (73)$$

We choose the positive constant c_2 such that

$$c_2 < \min \left\{ k_\Omega, \frac{4k_\Omega k_R \lambda_{\min}(J)^2}{k_\Omega^2 \lambda_{\max}(J) + 4k_R \lambda_{\min}(J)^2}, \sqrt{k_R \lambda_{\min}(J)} \right\},$$

which makes the matrix W_2 in (65) and the matrices M_{21}, M_{22} in (72) positive-definite. Therefore, we obtain

$$\lambda_{\min}(M_{21}) \|z_2\|^2 \leq \mathcal{V}_2 \leq \lambda_{\max}(M_{22}) \|z_2\|^2, \quad (74)$$

$$\dot{\mathcal{V}}_2 \leq -\lambda_{\min}(W_2) \|z_2\|^2. \quad (75)$$

Let $\beta_2 = \frac{\lambda_{\min}(W_2)}{\lambda_{\max}(M_{22})}$. Then, we have

$$\dot{\mathcal{V}}_2 \leq -\beta_2 \mathcal{V}_2. \quad (76)$$

Therefore, the zero equilibrium of the attitude tracking error e_R, e_Ω is exponentially stable. Using (71), this implies that

$$\begin{aligned} (2 - \psi_2) \lambda_{\min}(M_{21}) \Psi &\leq \lambda_{\min}(M_{21}) \|e_R\|^2 \\ &\leq \lambda_{\min}(M_{21}) \|z_2\|^2 \leq \mathcal{V}_2(t) \leq \mathcal{V}_2(0) e^{-\beta_2 t}. \end{aligned}$$

Thus, the attitude error function Ψ exponentially decreases. But, from (68), it is also guaranteed that $\Psi < 2$. This yields (14).

C. Proof of Proposition 2

The rotational dynamics (4), (5) are decoupled from the translational dynamics (2), (3). As the control moment and assumptions are identical to Proposition 1, all of the conclusions of Proposition 1 hold.

To show altitude tracking, we take the dot product of (3) with e_3 to obtain

$$m\ddot{x}_3 = mg - f e_3 \cdot R e_3.$$

Substituting (15) into this, we obtain the altitude error dynamics as follows:

$$m\ddot{x}_3 = -k_x(x_3 - x_{3d}) - k_v(\dot{x}_3 - \dot{x}_{3d}) + m\ddot{x}_{3d}.$$

It is clear that this second-order linear system is exponentially stable for positive k_x, k_v .

D. Proof of Proposition 3

We first derive the tracking error dynamics. Using a Lyapunov analysis, we show that the velocity tracking error is uniformly bounded, from which we establish exponential stability.

a) *Boundedness of e_R* : The assumptions of Proposition 3, namely (26), (33) imply satisfaction of the assumptions of Proposition 1, (12), (13), replacing the notation R_d by R_c . Therefore, the results of Proposition 1 can be directly applied throughout this proof. From (33), equation (67) can be replaced by

$$k_R \Psi(R(t), R_c(t)) \leq \mathcal{V}'_2(0) < k_R \psi_1. \quad (77)$$

Therefore, the *attitude error* function is bounded by

$$\Psi(R(t), R_d(t)) \leq \psi_1 < 1, \quad \text{for any } t \geq 0. \quad (78)$$

This implies that for the attitude always lies in the sublevel set $L_1 = \{R \in \text{SO}(3) \mid \Psi(R, R_c) < 1\}$. From (69), the *attitude error* is less than 90° . Similar to (71), we can show that

$$\frac{1}{2} \|e_R\|^2 \leq \Psi(R, R_c) \leq \frac{1}{2 - \psi_1} \|e_R\|^2. \quad (79)$$

b) *Translational Error Dynamics*: The time derivative of the position error is $\dot{e}_x = e_v$. The time-derivative of the velocity error is given by

$$m \dot{e}_v = m \ddot{x} - m \ddot{x}_d = m g e_3 - f R e_3 - m \ddot{x}_d. \quad (80)$$

Consider the quantity $e_3^T R_c^T R e_3$, which represents the cosine of the angle between $b_3 = R e_3$ and $b_{c_3} = R_c e_3$. Since $1 - \Psi(R, R_c)$ represents the cosine of the eigen-axis rotation angle between R_c and R , as discussed in (69), we have $1 > e_3^T R_c^T R e_3 > 1 - \Psi(R, R_c) > 0$. Therefore, the quantity $\frac{1}{e_3^T R_c^T R e_3}$ is well-defined. To rewrite the error dynamics of e_v in terms of the *attitude error* e_R , we add and subtract $\frac{f}{e_3^T R_c^T R e_3} R_c e_3$ to the right hand side of (80) to obtain

$$m \dot{e}_v = m g e_3 - m \ddot{x}_d - \frac{f}{e_3^T R_c^T R e_3} R_c e_3 - X, \quad (81)$$

where $X \in \mathbb{R}^3$ is defined by

$$X = \frac{f}{e_3^T R_c^T R e_3} ((e_3^T R_c^T R e_3) R e_3 - R_c e_3). \quad (82)$$

Let $A = -k_x e_x - k_v e_v - m g e_3 + m \ddot{x}_d$. Then, from (19), (23), we have $f = -A \cdot R e_3$ and $b_{c_3} = R_c e_3 = -A / \|A\|$, i.e. $-A = \|A\| R_c e_3$. By combining these, we obtain $f = (\|A\| R_c e_3) \cdot R e_3$. Therefore, the third term of the right hand side of (81) can be written as

$$\begin{aligned} -\frac{f}{e_3^T R_c^T R e_3} R_c e_3 &= -\frac{(\|A\| R_c e_3) \cdot R e_3}{e_3^T R_c^T R e_3} \cdot -\frac{A}{\|A\|} = A \\ &= -k_x e_x - k_v e_v - m g e_3 + m \ddot{x}_d. \end{aligned}$$

Substituting this into (81), the error dynamics of e_v can be written as

$$m \dot{e}_v = -k_x e_x - k_v e_v - X. \quad (83)$$

c) *Lyapunov Candidate for Translation Dynamics*: For a positive constant c_1 , let a Lyapunov candidate \mathcal{V}_1 be

$$\mathcal{V}_1 = \frac{1}{2} k_x \|e_x\|^2 + \frac{1}{2} m \|e_v\|^2 + c_1 e_x \cdot e_v. \quad (84)$$

The derivative of \mathcal{V}_1 along the solution of (83) is given by

$$\begin{aligned} \dot{\mathcal{V}}_1 &= k_x e_x \cdot e_v + e_v \cdot \{-k_x e_x - k_v e_v + X\} + c_1 e_v \cdot e_v \\ &\quad + \frac{c_1}{m} e_x \cdot \{-k_x e_x - k_v e_v + X\} \\ &= -(k_v - c_1) \|e_v\|^2 - \frac{c_1 k_x}{m} \|e_x\|^2 - \frac{c_1 k_v}{m} e_x \cdot e_v \\ &\quad + X \cdot \left\{ \frac{c_1}{m} e_x + e_v \right\}. \end{aligned} \quad (85)$$

We find a bound on X using (82) as follows. Since $f = \|A\| (e_3^T R_c^T R e_3)$, we have

$$\begin{aligned} \|X\| &\leq \|A\| \|(e_3^T R_c^T R e_3) R e_3 - R_c e_3\| \\ &\leq (k_x \|e_x\| + k_v \|e_v\| + B) \|(e_3^T R_c^T R e_3) R e_3 - R_c e_3\|. \end{aligned}$$

The last term $\|(e_3^T R_c^T R e_3) R e_3 - R_c e_3\|$ represents the sine of the angle between $b_3 = R e_3$ and $b_{c_3} = R_c e_3$, since

$$(b_{c_3} \cdot b_3) b_3 - b_{c_3} = b_3 \times (b_3 \times b_{c_3}).$$

From (70), $\|e_R\|$ represents the sine of the eigen-axis rotation angle between R_c and R . Therefore, we have $\|(e_3^T R_c^T R e_3) R e_3 - R_c e_3\| \leq \|e_R\|$. From (70), (78), it follows that

$$\begin{aligned} \|(e_3^T R_c^T R e_3) R e_3 - R_c e_3\| &\leq \|e_R\| = \sqrt{\Psi(2 - \Psi)} \\ &\leq \sqrt{\psi_1(2 - \psi_1)} \equiv \alpha < 1. \end{aligned}$$

Therefore, X is bounded by

$$\begin{aligned} \|X\| &\leq (k_x \|e_x\| + k_v \|e_v\| + B) \|e_R\| \\ &\leq (k_x \|e_x\| + k_v \|e_v\| + B) \alpha. \end{aligned} \quad (86)$$

Substituting this into (85),

$$\begin{aligned} \dot{\mathcal{V}}_1 &\leq -(k_v - c_1) \|e_v\|^2 - \frac{c_1 k_x}{m} \|e_x\|^2 - \frac{c_1 k_v}{m} e_x \cdot e_v \\ &\quad + (k_x \|e_x\| + k_v \|e_v\| + B) \|e_R\| \left\{ \frac{c_1}{m} \|e_x\| + \|e_v\| \right\} \\ &\leq -(k_v(1 - \alpha) - c_1) \|e_v\|^2 - \frac{c_1 k_x}{m} (1 - \alpha) \|e_x\|^2 \\ &\quad + \frac{c_1 k_v}{m} (1 + \alpha) \|e_x\| \|e_v\| \\ &\quad + \|e_R\| \left\{ k_x \|e_x\| \|e_v\| + \frac{c_1}{m} B \|e_x\| + B \|e_v\| \right\}. \end{aligned} \quad (87)$$

d) *Boundedness of $\|e_v\|$* : In the above expression for $\dot{\mathcal{V}}_1$, there is a third-order error term, namely $k_x \|e_R\| \|e_x\| \|e_v\|$. Here, we find a bound on $\|e_v\|$ to change this term into a second-order error term for the subsequent Lyapunov analysis. We consider a special case where the constants c_1 and k_x are zero. Define $\mathcal{V}'_1 = \mathcal{V}_1|_{c_1=k_x=0}$. From (84), (87), we have

$$\begin{aligned} \mathcal{V}'_1 &= \frac{1}{2} m \|e_v\|^2, \\ \dot{\mathcal{V}}'_1 &\leq -k_v (1 - \alpha) \|e_v\|^2 + B \|e_v\|. \end{aligned}$$

This implies that when $\|e_v\| > \frac{B}{k_v(1-\alpha)}$, the time derivative of $\|e_v\|$ is negative, and $\|e_v\|$ monotonically decreases. Therefore, $\|e_v\|$ is uniformly bounded as

$$\|e_v(t)\| \leq \max \left\{ \|e_v(0)\|, \frac{B}{k_v(1-\alpha)} \right\} \equiv e_{v_{\max}}. \quad (88)$$

e) *Lyapunov Candidate for the Complete System*:: Let $\mathcal{V} = \mathcal{V}_1 + \mathcal{V}_2$ be the Lyapunov candidate of the complete system.

$$\begin{aligned} \mathcal{V} &= \frac{1}{2}k_x\|e_x\|^2 + \frac{1}{2}m\|e_v\|^2 + c_1e_x \cdot e_v \\ &\quad + \frac{1}{2}e_\Omega \cdot Je_\Omega + k_R\Psi(R, R_d) + c_2e_R \cdot e_\Omega. \end{aligned} \quad (89)$$

Using (79), the bound of the Lyapunov candidate \mathcal{V} can be written as

$$z_1^T M_{11}z_1 + z_2^T M_{21}z_2 \leq \mathcal{V} \leq z_1^T M_{12}z_1 + z_2^T M'_{22}z_2, \quad (90)$$

where $z_1 = [\|e_x\|, \|e_v\|]^T$, $z_2 = [\|e_R\|, \|e_\Omega\|]^T \in \mathbb{R}^2$, and the matrices $M_{11}, M_{12}, M_{21}, M_{22}$ are given by

$$\begin{aligned} M_{11} &= \frac{1}{2} \begin{bmatrix} k_x & -c_1 \\ -c_1 & m \end{bmatrix}, \quad M_{12} = \frac{1}{2} \begin{bmatrix} k_x & c_1 \\ c_1 & m \end{bmatrix}, \\ M_{21} &= \frac{1}{2} \begin{bmatrix} k_R & -c_2 \\ -c_2 & \lambda_{\min}(J) \end{bmatrix}, \quad M'_{22} = \frac{1}{2} \begin{bmatrix} \frac{2k_R}{2-\psi_1} & c_2 \\ c_2 & \lambda_{\max}(J) \end{bmatrix}. \end{aligned}$$

Using (65), (87), (88), the time-derivative of \mathcal{V} is given by

$$\dot{\mathcal{V}} \leq -z_1^T W_1 z_1 + z_1^T W_{12} z_2 - z_2^T W_2 z_2, \quad (91)$$

where $W_1, W_{12}, W_2 \in \mathbb{R}^{2 \times 2}$ are defined as follows:

$$W_1 = \begin{bmatrix} \frac{c_1 k_x}{m} & -\frac{c_1 k_v}{2m}(1+\alpha) \\ -\frac{c_1 k_v}{2m}(1+\alpha) & k_v(1-\alpha) - c_1 \end{bmatrix}, \quad (92)$$

$$W_{12} = \begin{bmatrix} k_x e_{v_{\max}} + \frac{c_1 B}{m} & 0 \\ B & 0 \end{bmatrix}, \quad (93)$$

$$W_2 = \begin{bmatrix} \frac{c_2 k_R}{\lambda_{\max}(J)} & -\frac{c_2 k_\Omega}{2\lambda_{\min}(J)} \\ -\frac{c_2 k_\Omega}{2\lambda_{\min}(J)} & k_\Omega - c_2 \end{bmatrix}. \quad (94)$$

f) *Exponential Stability*: Under the given conditions (30), (31) of the proposition, all of the matrices $M_{11}, M_{12}, W_1, M_{21}, M_{22}, W_2$, and the Lyapunov candidate \mathcal{V} become positive-definite, and

$$\dot{\mathcal{V}} \leq -\lambda_{\min}(W_1)\|z_1\|^2 + \|W_{12}\|_2\|z_1\|\|z_2\| - \lambda_{\min}(W_2)\|z_2\|^2.$$

The condition given by (32) guarantees that $\dot{\mathcal{V}}$ becomes negative-definite. Therefore, the zero equilibrium of the tracking errors of the complete dynamics is exponentially stable.

E. Proof of Proposition 4

The given assumptions (34), (35) satisfy the assumption of Proposition 1, from which the tracking error $z_2 = [\|e_R\|, \|e_\Omega\|]$ is guaranteed to exponentially decrease, and to enter the region of attraction of Proposition 3, given by (26), (33), in a finite time t^* .

Therefore, if we show that the tracking error $z_1 = [\|e_x\|, \|e_v\|]$ is bounded in $t \in [0, t^*]$, then the tracking error $z = [z_1, z_2]$ is uniformly bounded for any $t > 0$, and it exponentially decreases for $t > t^*$. This yields exponential attractiveness.

The boundedness of z_1 is shown as follows. The error dynamics of e_v can be written as

$$m\dot{e}_v = mge_3 - fRe_3 - m\ddot{x}_d.$$

Let \mathcal{V}_3 be a positive-definite function of $\|e_x\|$ and $\|e_v\|$:

$$\mathcal{V}_3 = \frac{1}{2}\|e_x\|^2 + \frac{1}{2}m\|e_v\|^2.$$

Then, we have $\|e_x\| \leq \sqrt{2\mathcal{V}_3}$, $\|e_v\| \leq \sqrt{\frac{2}{m}\mathcal{V}_3}$. The time-derivative of \mathcal{V}_3 is given by

$$\begin{aligned} \dot{\mathcal{V}}_3 &= e_x \cdot e_v + e_v \cdot (mge_3 - fRe_3 - m\ddot{x}_d) \\ &\leq \|e_x\|\|e_v\| + \|e_v\|\|mge_3 - m\ddot{x}_d\| + \|e_v\|\|Re_3\|\|f\|. \end{aligned}$$

Using (25), (19), we obtain

$$\begin{aligned} \dot{\mathcal{V}}_3 &\leq \|e_x\|\|e_v\| + \|e_v\|B + \|e_v\|(k_x\|e_x\| + k_v\|e_v\| + B) \\ &= k_v\|e_v\|^2 + (2B + (k_x + 1)\|e_x\|)\|e_v\| \\ &\leq d_1\mathcal{V}_3 + d_2\sqrt{\mathcal{V}_3}, \end{aligned}$$

where $d_1 = k_v\frac{2}{m} + 2(k_x + 1)\frac{1}{\sqrt{m}}$, $d_2 = 2B\sqrt{\frac{2}{m}}$. Suppose that $\mathcal{V}_3 \geq 1$ for a time interval $[t_a, t_b] \subset [0, t^*]$. In this time interval, we have $\sqrt{\mathcal{V}_3} \leq \mathcal{V}_3$. Therefore,

$$\dot{\mathcal{V}}_3 \leq (d_1 + d_2)\mathcal{V}_3 \quad \Rightarrow \quad \mathcal{V}_3(t) \leq \mathcal{V}_3(t_a)e^{(d_1+d_2)(t-t_a)}.$$

Therefore, for any time interval in which $\mathcal{V}_3 \geq 1$, \mathcal{V}_3 is bounded. This implies that \mathcal{V}_3 is bounded for $0 \leq t \leq t^*$.

In summary, for any initial condition satisfying (34),(35), the tracking error converges to the region of attraction for exponential stability according to Proposition 3, and during that time period, tracking errors are bounded. Therefore, the zero equilibrium of the tracking error is exponentially attractive.

REFERENCES

- [1] M. Valenti, B. Bethke, G. Fiore, and J. How, "Indoor multi-vehicle flight testbed for fault detection, indoor multi-vehicle flight testbed for fault detection, isolation, and recovery," in *Proceedings of the AIAA Guidance, Navigation and Control Conference*, 2006.
- [2] P. Pounds, R. Mahony, and P. Corke, "Modeling and control of a large quadrotor robot," *Control Engineering Practice*, vol. 18, pp. 691–699, 2010.
- [3] G. Hoffmann, H. Huang, S. Waslander, and C. Tomlin, "Quadrotor helicopter flight dynamics and control: Theory and experiment," in *Proceedings of the AIAA Guidance, Navigation, and Control Conference*, 2007, AIAA 2007-6461.
- [4] P. Castillo, R. Lozano, and A. Dzul, "Stabilization of a mini rotorcraft with four rotors," *IEEE Control System Magazine*, pp. 45–55, 2005.
- [5] Mikrokopter. [Online]. Available: <http://www.mikrokopter.de/>
- [6] Microdrone-bulgaria. [Online]. Available: <http://www.microdrones-bulgaria.com/>
- [7] Dragonfly innovations. [Online]. Available: <http://www.draganfly.com/>
- [8] S. Bouabdalla, P. Murrieri, and R. Siegward, "Towards autonomous indoor micro VTOL," *Autonomous Robots*, vol. 18, no. 2, pp. 171–183, 2005.
- [9] E. Nice, "Design of a four rotor hovering vehicle," Master's thesis, Cornell University, 2004.
- [10] N. Guenard, T. Hamel, and V. Moreau, "Dynamic modeling and intuitive control strategy for an X4-flyer," in *Proceedings of the IEEE International Conference on Control and Application*, 2005.
- [11] S. Bouabdalla and R. Siegward, "Backstepping and sliding-mode techniques applied to an indoor micro quadrotor," in *Proceedings of the IEEE International Conference on Robotics and Automation*, 2005, pp. 2259–2264.
- [12] V. Jurdjevic, *Geometric Control Theory*. Cambridge University, 1997.

- [13] A. Bloch, *Nonholonomic Mechanics and Control*, ser. Interdisciplinary Applied Mathematics. Springer-Verlag, 2003, vol. 24.
- [14] F. Bullo and A. Lewis, *Geometric control of mechanical systems*, ser. Texts in Applied Mathematics. New York: Springer-Verlag, 2005, vol. 49, modeling, analysis, and design for simple mechanical control systems.
- [15] S. Bhat and D. Bernstein, "A topological obstruction to continuous global stabilization of rotational motion and the unwinding phenomenon," *Systems and Control Letters*, vol. 39, no. 1, pp. 66–73, 2000.
- [16] D. Maithripala, J. Berg, and W. Dayawansa, "Almost global tracking of simple mechanical systems on a general class of Lie groups," *IEEE Transactions on Automatic Control*, vol. 51, no. 1, pp. 216–225, 2006.
- [17] D. Cabecinhas, R. Cunha, and C. Silvestre, "Output-feedback control for almost global stabilization of fully-actuated rigid bodies," in *Proceedings of IEEE Conference on Decision and Control*, 3583–3588, Ed., 2008.
- [18] N. Chaturvedi, N. H. McClamroch, and D. Bernstein, "Asymptotic smooth stabilization of the inverted 3-D pendulum," *IEEE Transactions on Automatic Control*, vol. 54, no. 6, pp. 1204–1215, 2009.
- [19] A. Tayebi and S. McGilvray, "Attitude stabilization of a VTOL quadrotor aircraft," *IEEE Transactions on Control System Technology*, vol. 14, no. 3, pp. 562–571, 2006.
- [20] M. Oishi and C. Tomlin, "Switched nonlinear control of a VSTOL aircraft," in *Proceedings of IEEE Conference on Decision and Control*, 1999, pp. 2685–2690.
- [21] R. Ghosh and C. Tomlin, "Nonlinear inverse dynamic control for mode-based flight," in *Proceedings of the AIAA Guidance, Navigation and Control Conference*, 2000.
- [22] M. Oishi and C. Tomlin, "Switching in nonlinear minimum phase systems: Applications to a VSTOL aircraft," in *Proceedings of American Control Conference*, 2002.
- [23] P. Crouch, "Spacecraft attitude control and stabilizations: applications of geometric control theory to rigid body models," *IEEE Transactions on Automatic Control*, vol. 29, no. 4, pp. 321–331, 1984.
- [24] Z. Qu, *Robust Control of Nonlinear Uncertain Systems*. New York, NY, USA: John Wiley & Sons, Inc., 1998.
- [25] T. Lee, M. Leok, and N. McClamroch, "Control of complex maneuvers for a quadrotor UAV using geometric methods on $SE(3)$," arXiv, 2010. [Online]. Available: <http://arxiv.org/abs/1003.2005>